Modern Physics Letters B, Vol. 19, No. 15 (2005) 697–706

World Scientific
www.worldscientific.com

MODELING OF ELECTRICAL BEHAVIOR OF $La_{0.7}Ca_{0.3}MnO_3$ CERAMIC USING IMPEDANCE SPECTROSCOPY

VINOD KUMAR[*,¶], O. P. THAKUR[†], LAKSHMAN PANDEY[*,‖], A. P. GUIMARAES[‡], ANUBHA GOEL[§], OM PARKASH[§] and DEVENDRA KUMAR[§]

[*] *Department of Physics, Rani Durgavati University, Jabalpur-482001, India*
[†] *Electroceramics Division, Solid State Physics Laboratory, Timarpur, Lucknow Road, Delhi-110054, India*
[‡] *Brazilian Centre for Physical Research (CBPF), Centro Brasileiro de Pesquisas Fisicas, Rua Dr. Xavier Sigaud, 150, 22290-180 Urca, Rio de Janerio, RJ, Brazil*
[§] *Department of Ceramic Engineering, Institute of Technology, Banaras Hindu University, Varnasi-221005, India*
[¶] *vinodkp@sancharnet.in*
[‖] *pandeyl@hotmail.com*

Received 3 January 2005

The ceramic system $La_{0.7}Ca_{0.3}MnO_3$ was prepared by solid state method and impedance measurements were carried out as a function of frequency (100 Hz – 1 MHz) in the temperature range 303–529 K. An equivalent circuit model that represented the data well was arrived at by comparing the experimental plots with computer simulated complex immittance spectra of model circuits. It consisted of three parallel RC circuits connected in series indicating the presence of three processes present in the system. The resistances are found to follow the behavior $R = R_0 \exp(E/kT)$. The values of activation energy E for these are obtained.

Keywords: Impedance; immittance; spectroscopy; electronic ceramics; CMR.

1. Introduction

The ceramic system $La_{1-x}Ca_xMnO_3$ is known to possess colossal magnetoresistance (CMR) behavior below 268 K and has been subject to intense research activities in the last few years due to its great potential for technological applications.[1] This material shows CMR behavior in polycrystalline form as well, which makes it a very important ceramic for possible device development owing to ease of preparation and processing. The temperature T_m at which magnetoresistance (MR) is maximum is generally close to the ferromagnetic transition temperature ($T_c \sim 268$ K).[1] Attempts have been made to obtain even larger MR and higher values of T_c close to room temperature by making substitutions at La and Mn sites.[2] The magnetoresistance, defined as $(R(0) - R(H))/R(H)$, where $R(H)$ is the resitivity in a

*Corresponding authors.

magnetic field H, exceeds 100000% in some of the materials.[3] This behavior has been termed as *colossal magnetoresistance* (CMR). The lanthanum manganites exhibit a metallic conductivity below T_c and an activated temperature dependence of conductivity above T_c.[4] It has been proposed that CMR appears due to strong coupling among charge, spin, orbital and lattice degrees of freedom and distortions of local entities and clusters with the bulk properties.[5,6] Local probes such as NMR have been extensively used to understand these interactions and the nature of the clusters.[4,5,7–10] However for clear understanding of the role of the clusters and distortions, study of local behavior as well as of the bulk is required. Also the study of bulk electrical behavior is useful in achieving tailor-made properties and desired device applications. Extensive literature is available regarding the transport studies in doped and phase separated lanthanum and mixed valence manganites.[1,11–16] It has been indicated that electron transport at $T > T_c$ is activated and metal-like resistivity behavior $\rho d\rho/dt > 0$, where $T < T_c$, is related to the occurrence of a long range ferromagnetic state arising from the Mn^{3+}-O-Mn^{4+} interaction and GMR is directly linked to the presence of Mn^{4+} in adequate proportion. Higher values of conductivity have been achieved by preparing Ag-containing CMR nano composites.[13]

It has been inferred using impedance spectroscopy that some physical grains of $La_{0.6}Y_{0.1}Ca_{0.3}MnO_3$ may have phases or clusters with different spin dynamics and transport mechanisms.[16] Transport properties of $La_{0.6}Y_{0.1}Ca_{0.3}MnO_3$ compounds with different interfaces have been studied utilizing impedance spectroscopy.[12] Also, impedance spectroscopic evidence of the phase separation in $La_{0.3}Pr_{0.4}Ca_{0.3}MnO_3$ has been presented.[11] It has been shown that below T_c, $La_{1-x}Ca_xMnO_3$ with $0.2 < x < 0.5$ exhibit ferromagnetism and a metallic conductivity owing to the double exchange interaction between Mn^{3+}—Mn^{4+} pairs. The Mn^{3+} when substituted by Ca^{2+} ions gives rise to a hole at the Mn site and valence compensation yields the Mn^{4+} ions. It has also been suggested that the Mn^{3+}—Mn^{4+} pairs are confined in a small region of the size ~ 30 Å and two phases coexist with very different Mn ions spin dynamics.[11,17] In order to understand the behavior of this system above T_c impedance spectroscopic studies have been carried out and an equivalent circuit model representing the behavior of the system is presented in this paper.

In this paper we report impedance spectroscopic study of the ceramic system $La_{0.7}Ca_{0.3}MnO_3$ in the frequency range 100 Hz – 1 MHz and at temperatures above T_c and in the range 303–529 K. The impedance data is analyzed to obtain an equivalent circuit model by comparing the experimental plots with computer-simulated complex immittance spectra of model equivalent circuit. In the next section we give the experimental method for the preparation of the sample followed by a brief overview of the equivalent circuit modeling, the result and discussion.

2. Experiment

The sample with composition $La_{0.7}Ca_{0.3}MnO_3$ was prepared by solid state ceramic method using AR grade $CaCO_3$, MnO_2 and La_2O_3 as starting materials. An appropriate amount was ball-milled using zirconia balls in distilled water and then calcined at 800°C for 4 hours. The powder was ball-milled again and calcined at 850°C for 4 hours. Calcined powder was isostatically pressed in pellet form at a pressure of 200 MPa using cold press supplied by M/S Autoclave Engineers. Cold isostatic process gives better homogeneity of the green pellets. These pellets were sintered at 1250°C for 3 hours in air.

The formation of single phase compound was checked by X-ray diffraction technique. XRD patterns were recorded using Phillips powder diffractometer with Cu-Kα radiation in a wide range of 2θ ($10 \leq 2\theta \leq 80$) at a scanning rate of 2°/min. For electrical characterization, sintered pellets were ground to a thickness of 0.5 mm. Both the faces of the polished sample were gold sputtered.

Measurement of capacitance (C) and dissipation factor ($\tan\delta$) was carried out by a HP4248A LCR meter interfaced with a computer as a function of frequency (100 Hz – 1 MHz) in the temperature range 303–529 K. Heating was maintained at 1°C/min and data was recorded automatically. The dielectric data obtained for different temperatures was used to determine the real and imaginary parts of complex immittance functions, viz. impedance ($Z^* = Z' - jZ''$), admittance ($Y^* = 1/Z^* = Y' + jY''$), permittivity ($\varepsilon^* = (j\omega C_0 Z)^{-1} = \varepsilon' - j\varepsilon''$) and dielectric modulus ($M^* = (\varepsilon^*)^{-1} = j\omega C_0 Z^* = M' + jM''$). Impedance and modulus spectroscopic techniques were used to find out the equivalent circuit model that represents the electrical behavior of the CMR samples. Different resistive (R's) and capacitive (C's) components of the modeled equivalent circuit were determined by a complex nonlinear least squares (CNLS) fitting program using IMPSPEC.BAS software developed by Pandey.[18]

3. Equivalent Circuit Models

Equivalent circuit models and their simulated spectroscopic and complex plane plots have been discussed earlier by various workers,[19–32] however, for a ready reference, a brief overview is presented below and spectra for some relevant models are simulated. A RC circuit has one time constant and can conveniently be used to represent one charge transfer/relaxation process in the material. The real and imaginary parts of the complex impedance $Z^* = Z' - jZ''$ of a parallel RC circuit is given by

$$Z' = \frac{R}{1 + (\omega RC)^2}, \qquad Z'' = \frac{\omega R^2 C}{1 + (\omega RC)^2} \tag{1}$$

where $\omega = 2\pi f$, f being the frequency of measurement. It is seen that Z' and Z'' satisfy the relation

$$\left(Z' - \frac{R}{2}\right)^2 + Z''^2 = \left(\frac{R}{2}\right)^2, \tag{2}$$

which is the equation of a circle. Since Z' and Z'' are positive as given by Eq. (1), the plot of Z'' versus Z' is a semicircular arc with center at $(R/2, 0)$ and radius $R/2$. The point ($Z' = R$, $Z'' = 0$) corresponds to $\omega = 0$, i.e. dc resistance. Also, Eq. (1) tells that the maximum value of Z' occurs at $\omega RC = 1$. Thus if Z' and Z'' for a system are measured experimentally and Z'' versus Z' plot is semicircular, the system can be represented, to begin with, by a parallel RC circuit. The value of R is obtained by the low-frequency intercept of the arc with Z'-axis and C is obtained by noting the frequency where Z'' is maximum and using $\omega RC = 1$. The value of C can be alternatively obtained by analyzing the experimental data using other interrelated immittance functions mentioned in the previous sections. The real and imaginary part M' and M'' of the dielectric modulus $M^* = (1/\varepsilon^*)$ given by

$$M' = \omega C_0 Z'' \qquad \text{and} \qquad M'' = \omega C_0 Z' \,,$$

where C_0 is the capacitance of the empty cell used to house the sample, satisfy the relation

$$\left(M' - \frac{C_0}{2C}\right)^2 + M'' = \left(\frac{C_0}{2C}\right)^2 . \tag{3}$$

Also as $\omega \to \infty$, $M' = C_0/C$ and $M'' = 0$ indicating that a plot of M'' versus M' would be a semicircular arc with center at $(C_0/2C, 0)$ and high frequency intercept at C_0/C. Thus knowing C_0, the values of R and C can be directly obtained from the complex plane plots of Z'' versus Z' and M'' versus M'. A series RC circuit may also be chosen for the model as series and parallel representations are equivalent. However Y'' versus Y' and ε'' versus ε' plots will then be useful.[24]

When two charge transfer processes are present in the material then a series combination of two parallel RC circuits having time constants R_1C_1 and R_2C_2 may be considered as a representative model as shown in Fig. 1(a). The Z'' versus Z' plot may contain two distinct arcs or may appear slightly depressed depending on the ratios R_2C_2/R_1C_1 and R_2/R_1. A slightly depressed semicircular arc indicates the presence of distribution in time constant or the presence of at least two processes whose time constants are close to each other within a factor of 3 [see Fig. 1(b)]. For a given experimentally observed Z'' versus Z' plot, approximate values of R_2C_2/R_1C_1 and R_2/R_1 can be obtained by comparing the experimental plots with simulated ones.

The simulated plot for Z'' versus Z', M'' versus M', etc., are given in Ref. 24 for various values of R_2C_2/R_1C_1 and R_2/R_1 and it has been concluded that two plots, viz. Z'' versus Z' and M'' versus M' plots, or the plots Y'' versus Y' and ε'' versus ε', should be looked at for choosing a suitable model.[24] Plots of Z'' versus Z' and M'' versus M' for a few values of R_2C_2/R_1C_1 and R_2/R_1 are given in Figs. 1(a)–1(e) for a ready reference. Choosing a model based on only one plot of the four immittance functions may be erroneous.[24]

The overall dielectric properties of a ceramic system would arise due to contributions from intragrain (i.e. grain, g) intergrain (i.e. grain boundary, gb) and

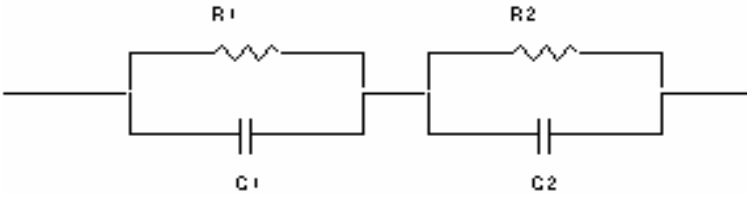

(a)

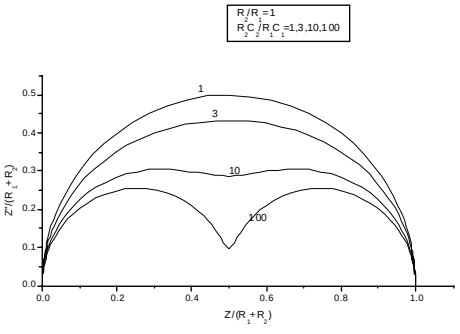

(b)

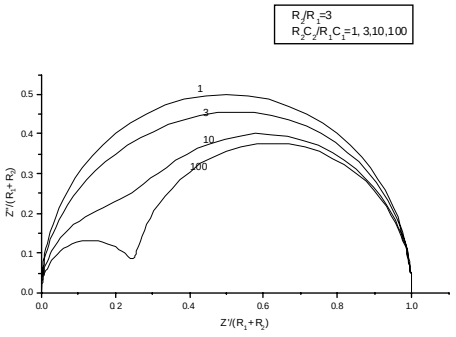

(c)

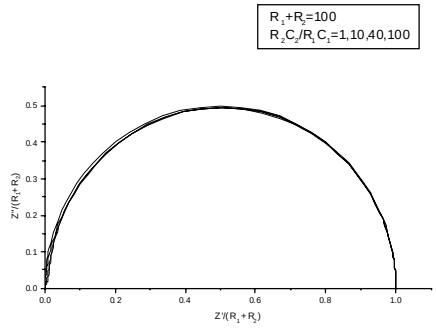

(d)

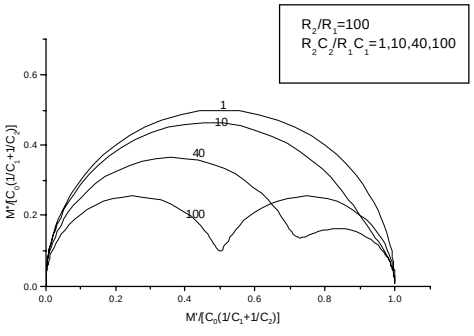

(e)

Fig. 1. (a) Model comprising two parallel RC circuits connected in series. (b) Normalized $Z''/(R_1 + R_2)$ versus $Z'/(R_1 + R_2)$ plots for various values of R_2C_2/R_1C_1 and $R_2/R_1 = 1$. (c) Normalized $Z''/(R_1 + R_2)$ versus $Z'/(R_1 + R_2)$ plots for various values of R_2C_2/R_1C_1 and $R_2/R_1 = 3$. (d) Normalized $Z''/(R_1 + R_2)$ versus $Z'/(R_1 + R_2)$ plots for various values of R_2C_2/R_1C_1 and $R_2/R_1 = 100$. (e) Normalized $M''/[C_0(1/C_1 + 1/C_2)]$ versus $M'/[C_0(1/C_1 + 1/C_2)]$ plots for various values of R_2C_2/R_1C_1 and $R_2/R_1 = 100$.

electrode contributions. A suitable simple model representing this would comprise three parallel RC circuits connected in series as shown in Fig. 2(a).

The Z' and Z'' are given as

$$Z' = \frac{R_1}{1 + (\omega R_1 C_1)^2} + \frac{R_2}{1 + (\omega R_2 C_2)^2} + \frac{R_3}{1 + (\omega R_3 C_3)^2},$$

$$Z'' = \frac{\omega C_1 R_1}{1 + (\omega R_1 C_1)^2} + \frac{\omega C_2 R_2}{1 + (\omega R_2 C_2)^2} + \frac{\omega C_3 R_3}{1 + (\omega R_3 C_3)^2}.$$

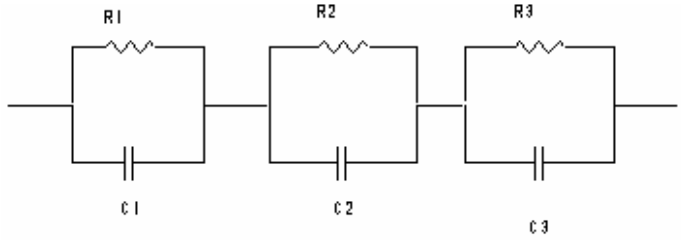

(a)

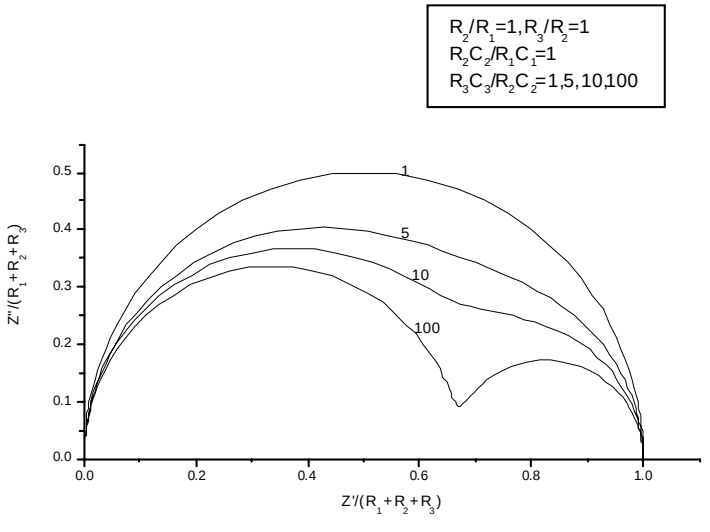

(b)

Fig. 2. (a) Model comprising three parallel RC circuits connected in series. (b) Normalized $Z''/(R_1 + R_2 + R_3)$ versus $Z'/(R_1 + R_2 + R_3)$ plots for various ratios of time constants and $R_2/R_1 = 1$, $R_3/R_2 = 1$.

Simulated typical plots are shown in Fig. 2(b). For other ratios of the time constants, skewed arcs are obtained. It is worth mentioning that the presence of a series resistance in the model gives rise to a positive shift on the Z'-axis in the Z'' versus Z' plot and a steeply rising branch at higher frequency in the M'' versus M' plot.

Similarly the presence of a series capacitance would yield a steeply rising low frequency branch in the Z'' versus Z' plot and a shift on the M' axis in M'' versus M' plot at low frequency.[24,29] When parallel RC circuits are present and connected in series as shown in Fig. 2(a) both the Z'' versus Z' and M'' versus M' plots would touch the origin and would meet the real axis again at low frequency ($\omega > 0$) for the Z-plot and high frequency ($\omega \to \infty$) for M-plots. If the Z'' versus Z' plot is a straight line inclined to the Z'-axis, the presence of constant phase angle element (CPE) connected in series is indicated.[21] These remarks are very useful in choosing a representative equivalent circuit model.

4. Result and Discussion

A typical Z'' versus Z' plot for the system $La_{0.7}Ca_{0.3}MnO_3$, is given in Fig. 3(a) and the corresponding spectroscopic plots are shown in Fig. 3(b). The Z'' versus Z' plot of Fig. 3(a) is not a clear semicircle arc, it meets the origin at high frequency and has an intercept on the Z'-axis at the low frequency end. The corresponding M'' versus M' plot also has an almost similar appearance [Fig. (4)]. Following the discussion presented in the previous paragraph, the presence of series R or series C in the equivalent circuit model is ruled out and a suitable simple equivalent circuit model would comprise three parallel RC circuits connected in series. A quick look

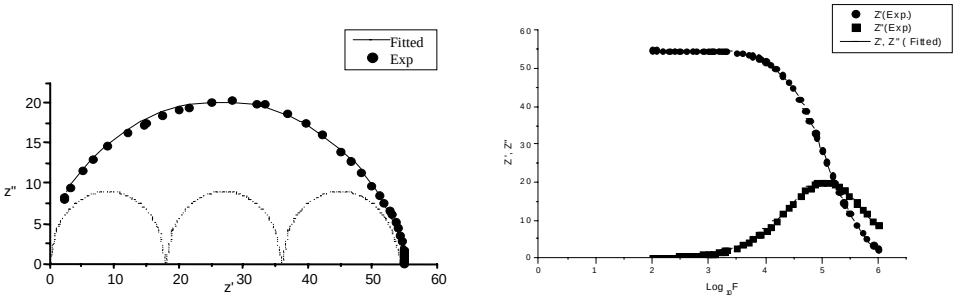

(a) (b)

Fig. 3. (a) Z'' versus Z' and (b) Z' and Z'' versus $\log_{10}$ (F) plots for the ceramic $La_{0.7}Ca_{0.3}MnO_3$ at 23°C. (• indicate experimental values; the *solid line* represents values calculated using CLNS fitting for the model shown in Fig. 2(a); the *dotted lines* of the tentative curves indicate the independent contributions of R_1, C_1, R_2, C_2, and R_3, C_3.)

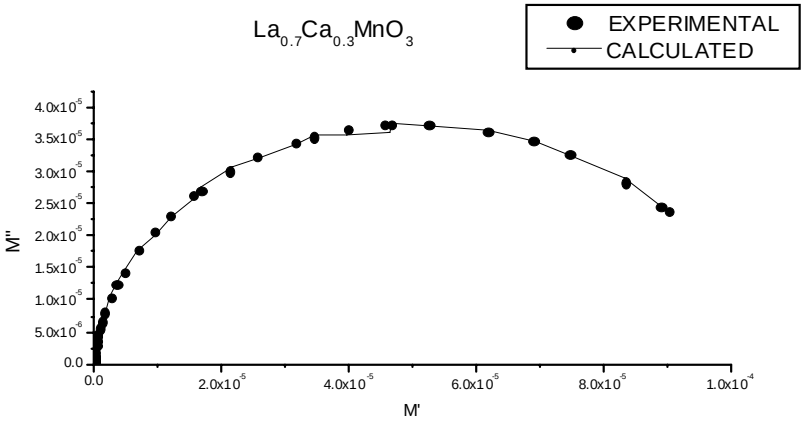

Fig. 4. M'' versus M' plot for $La_{0.7}Ca_{0.3}MnO_3$ at temperature 23°C. [• represent experimental values; the *solid line* respresents values calculated using CLNS fitting for the model shown in Fig. 2(a).]

at the experimental plot of Fig. 3(a) and simulated plot of Fig. 2(b) reveals that we can chose $R_1 \sim R_2 \sim R_3 \sim 18\ \Omega$ and $C_1 \approx 2.2 \times 10^{-8}$ F, $C_2 \approx 8.8 \times 10^{-8}$ F, $C_3 \approx 3.5 \times 10^{-7}$ F. Tentative independent arcs corresponding to such a situation are shown by dotted curves in Fig. 3(a). The exact values of R's and C's were obtained using the complex nonlinear least squares (CNLS) fitting program using IMPSPEC.BAS software developed by Pandey[18] using the above values as initial guesses. These values at room temperature are: $R_1 = (16.6 \pm 0.1)\,\Omega$, $C_1 = (2.6 \pm 0.04)$ F, $R_2 = (30.6 \pm 0.1)\,\Omega$, $C_2 = (6.21 \pm 0.13)$ F, $R_3 = (7.59 \pm 0.09)\,\Omega$, $C_3 = (1.51 \pm 0.04)$ F.

R_1, R_2 and R_3 follow the Arhenius-type behavior $R = R_0 \exp(E/kT)$ and the values of the corresponding activation energies are (152 ± 14) meV, (219 ± 16) meV and (272 ± 30) meV.

From above analysis the total dc resistance of the system was found to be $(54.8 \pm 0.1)\,\Omega$. This agrees very well with the value 54.4 Ω obtained from direct dc measurement. Also it was found that the directly measured dc resistance obeyed Ohm's law indicating that the electrode contact was Ohmic and the contact electrode contribution to the overall impedance behavior may be represented by a series resistance in the equivalent circuit. But such a situation should have yielded a shifted semicircular arc in the Z'' versus Z' plot. Therefore we believe that the three processes indicated by R_1C_1, R_2C_2 and R_3C_3 are present in the material itself. We attribute this to the two processes present in the grain and one process in grain boundary. Some workers have argued that two processes corresponding to ferromagnetic and antiferromagnetic regions (clusters) are present in the grains of $La_{1-x}Ca_xMnO_3$-type materials below T_c, with not so much contribution from *gb*.[12,17] The work presented in this paper indicates that two processes are present in the grains above T_c, and that there is also some *gb* contribution. The origin of the three processes present above and below T_c are to be further investigated.

5. Conclusions

Impedance spectroscopic studies have been carried out in $La_{1-x}Ca_xMnO_3$ above T_c in the temperature range 300–530 K. It is found that an equivalent circuit comprising three parallel RC circuits connected in series represents the data well. It has been concluded that two processes present in the grain and one present in the *gb* contribute to the overall impedance behavior of these manganites.

Acknowledgments

Financial support received from the Department of Science and Technology, Government of India (Project No. SP/S2/M-28/98) is gratefully acknowledged. V.K. is grateful for the Junior Research Fellowship in the project.

References

1. R. Mahendiran, S. K. Tiwary, A. K. Roychoudhry, T. V. Ramakrishnan, R. Mahesh, N. Rangavittal and C. N. R. Rao, *Phys. Rev.* **B53** (1996) 3348.
2. J. M. De Teresa, M. R. Ibarra, J. Blasco, J. Garcia, C. Marquina, P. A. Algarabel, Z. Arnold, K. Kamanev, C. Ritter and R. Von Helmolt, *Phys. Rev.* **B54** (1996) 1187.
3. S. Jin, H. M. O'Bryan, T. H. Tiefel, M. McCormack and W. W. Rhodes, *Appl. Phys. Lett.* **66** (1995) 382.
4. Cz. Kapusta, P. C. Riedi, W. Kocemba, G. J. Tomka, M. R. Ibarra, J. M. De Teresa, M. Viret and J. M. D. Coey, *J. Phys: Condens. Matter* **11** (1999) 4079.
5. K. E. Sakai, C. P. Slitcher, P. Lin, M. Jaime and M. B. Salamon, *Phys. Rev.* **B59** (1999) 9382.
6. A. H. Millis, *Nature* (*London*) **392** (1998) 147.
7. G. Allodi, R. De Renzi and G. Guidi, *Phys. Rev.* **B57** (1998) 1024.
8. G. Papavassiliou, M. Fardis, M. Belesi, M. Pissas, I. Panagiotopoulos, G. Kallias, D. Niarchos, C. Dimitropoulos and J. Dolinsek, *Phys. Rev.* **B59** (1999) 6390.
9. K. Kumagai, A. Iwai, Y. Tomioka, H. Kuwahara, Y. Tokura and A. Yakubovskii, *Phys. Rev.* **B59** (1999) 97.
10. Cz. Kapusta, P. C. Riedi, M. Sikora and M. R. Ibarra, *Phys. Rev. Lett.* **84** (2000) 4216.
11. J. A. Souza, R. F. Jardim, R. Muccillo, E. N. S. Muccillo, M. S. Torikachvili and J. J. Neumeire, *J. Appl. Phys.* **89** (2001) 6636.
12. F. C. Fonseca, J. A. Souza, R. F. Jardim, R. Muccillo, E. N. S. Muccillo, D. Gouvea, M. H. Jung and A. H. Lacerda, *Phys. Status Solidi* **A199** (2003) 255.
13. S. Pal, A. Bannerjee, S. Chatterjee, A. K. Nigam, B. K. Chaudhuri and H. D. Yang, *J. Appl. Phys.* **94** (2003) 3485.
14. A. S. Carneiro, F. C. Fonseca, R. Jardin and T. Kimura, *J. Appl. Phys.* **93** (2003) 8074.
15. F. C. Fonseca, A. S. Carneiro, R. F. Jardin, J. R. O'Brien and T. Kimura, *J. Appl. Phys.* **95** (2004) 7085.
16. F. C. Fonseca, J. A. Souza, R. F. Jardin, R. Muccillo, E. N. S. Muccillo, D. Gouvea, M. H. Jung and A. H. Lacerda, *J. Eur. Ceram. Soc.* **24** (2004) 1271.
17. R. H. Heffner, J. E. Sonier, D. E. MacLaughlin, G. J. Nieuwenhuys, G. Ehlers, F. Mezei, S. W. Cheong, J. S. Gardner and H. Roder, *Phys. Rev. Lett.* **85** (2000) 3285.
18. L. Pandey, *Workshop on Use of Computers in Teaching Physics*, partly sponsored by ICTP, Jabalpur, India (1992).
19. I. M. Hodge, M. D. Ingam and A. R. West, *Electronal. Shem.* **74** (1976) 125.
20. A. Hooper, *J. Phys.* **D10** (1977) 1487.
21. J. R. Macdonald, *Impedance Spectroscopy* (John Wiley and Sons, NY, 1987).
22. A. K. Jonscher, *Dielectric Relaxation in Solids* (Chelsa Dielectric Press, London, 1983).
23. R. Von Hipple, *Dielectrics and Waves* (John Wiley and Sons, NY, 1954).
24. L. Pandey, O. Parkash, R. K. Katare and D. Kumar, *Bull. Mater. Sci.* **18** (1995) 563.
25. O. Parkash, L. Pandey, H. S. Tiwari, V. B. Tare and D. Kumar, *Ferroelectrics* **102** (1990) 203.
26. O. Parkash, H. S. Tiwari, V. B. Tare and D. Kumar, *J. Am. Ceram. Soc.* **75** (1992) 3141.
27. L. Pandey, O. Parkash and D. Kumar, *Ind. J. Pure Appl. Phys.* **34** (1996) 28.
28. R. K. Katare, Application of impedance spectroscopy in the study of electronic ceramics, Ph.D. thesis, Rani Durgavati University, Jabalpur, India (1997).

29. L. Pandey, R. K. Katare, O. Parkash, D. Kumar and O. P. Thakur, *Ind. J. Pure Appl. Phys.* **36** (1998) 228.
30. R. K. Katare, L. Pandey, R. K. Dwivedi, O. Parkash and D. Kumar, *Ind. J. Eng. Mater. Sci.* **6** (1999) 34.
31. R. K. Katare, L. Pandey, O. P. Thakur, O. Parkash and D. Kumar, *Mod. Phys. Lett.* **B17** (2003) 339.
32. O. P. Thakur, D. Kumar, O. Parkash and L. Pandey, *J. Ceram. Process. Res.* **5** (2004) 106.
33. L. Pandey, R. K. Katare, O. Parkash and D. Kumar, *Bull. Mater. Sci.* **20** (1997) 933.